Organic & Biomolecular Chemistry

Accepted Manuscript

ROYAL SOCIETY OF CHEMISTRY

www.rsc.org/obc

Journal Name Organic & Biomolecular Chemistry Dynamic Article Links ►

Cite this: DOI: 10.1039/c0xx00000x

www.rsc.org/xxxxxx

ARTICLE TYPE

Effects of side chains on DNA binding, cell permeability, nuclear localization and cytotoxicity of 4-Aminonaphthalimides

Jin Zhou[a,b], Ang Chang[a,c], Linlin Wang[a], Ying Liu[a,b], Xiangjun Liu[a], Dihua Shangguan*[a]

Received (in XXX, XXX) Xth XXXXXXXXX 20XX, Accepted Xth XXXXXXXXX 20XX

DOI: 10.1039/b000000x

Nucleic acid binding molecules have been extensively explored for nucleic acid assay, nuclear imaging, and antitumor and antivirus therapies. Most of these molecules usually bear positive charges to enhance their binding affinity. However, the *in vivo* applications of them are limited by poor membrane permeability and lack of selectivity to nucleic acids. Here we describe the effects of positive charged side chains (including aminoethyl, dimethylaminopropyl and guanidinoethyl) on the DNA binding ability, cell permeability, cellular localization and cytotoxicity of 4-aminonaphthalimides, a class of DNA-intercalating agents and fluorophores. The synthesized 4-aminonaphthalimides have strong binding ability to duplex DNA, and can be used as pre-staining dyes for gel electrophoresis of DNA and RNA. When entering into cells, they rapidly concentrate in cell nuclei, especially in nucleoli. The guanidinoethyl side chains increase the binding ability to nucleic acids, but do not favour the cell permeability and cytotoxicity; dimethylaminopropyl groups enhance the cell permeability and cytotoxicity of 4-aminonaphthalimides. These results suggest the potential applications of 4-aminonaphthalimides in nucleic acid assay, nuclear imaging, and provide useful information for the molecular design of DNA-binding drugs and fluorescent probes.

Introduction

The organic molecules that bind to nucleic acids have been extensively developed for nucleic acid assay, fluorescent cellular imaging, as well as antitumor and antivirus therapies[1]. A large percentage of the chemotherapeutic anticancer agents currently used are DNA-binding drugs[2]. However, the applications of many of the DNA-binding molecules in live cells and in vivo are limited by their poor membrane permeability and lack of selectivity to nucleic acids. Therefore the development of new organic molecules with high cell permeability and nucleic acid selectivity has attracted extensive attention, e.g. bis-benzimidazole based dyes that are not only cell permeable, but can also discriminate between the duplex DNA and other higher order DNA forms[3]. The investigation on the DNA binding ability, cell permeability, cellular localization and cytotoxicity of DNA-binding molecules will provide useful information for the design of new DNA-binding drug and probe for the cellular imaging.

Since DNA is mainly localized in cell nucleus, some of DNA binding molecules are used as fluorescent nuclear stains and widely employed in cell life cycle analysis and nuclear imaging[4]. The commonly used nuclear stains include following two categories: 1) TO (thiazole orange), SYTOX, EB (Ethidium bromide) and PI (propidium iodide) dyes, which are lack of membrane permeability and used for dead cell staining; 2) SYTO, DAPI (4, 6-diamino-2-phenyl indole) and Hoechst, which have good cell permeability and can be used for live cell staining. Among these dyes, DAPI and Hoechst require ultraviolet excitation, which can result in cellular damage.[5] SYTO stains can be excited by visible and near-infrared radiation, unfortunately they have low selectivity to cell nucleus[6]. The choice of nuclear dye is still a thorny issue, many efforts have been made to design new nuclear dyes[4d], such as, DRAQ5 (cell-permeant anthraquinone dye)[7]; DEAB-TO-3(TO-3 analogue)[5], and LIr1 (iridium(III) complex)[6]. Usually, the requirements for good nuclear probes are: long-wavelength excitation/emission, high DNA selectivity, live-cell permeability and significant dynamic changes of fluorescence properties, such as fluorescence enhancement or wavelength shift.

Naphthalimide derivatives, as a class of DNA-intercalating agents, have been extensively explored as antitumor agents. Several naphthalimides (such as amonafide, mitonafide,bisnafide and elinafide) have reached clinical trials[8] In the family of naphthalimides, 3- and 4-aminonaphthalimides show strong absorption and emission in the visible region, with high photostability and large Stokes' shift. These advantageous optical properties are due to the internal charge transfer (ICT) nature, which is caused by their electronic push−pull structure[9]. Therefore, 4-aminonaphthalimides have been widely developed as fluorescent and colorimetric sensors for ion detection[10] and cellular imaging of pH and bioactive molecules (thiol, H_2O_2 and so on)[11]. However, 4-aminonaphthalimides have been rarely investigated as fluorescent probes for nucleic acid staining in vitro or cell nucleus staining in vivo. This may due to the small

dynamic changes of their optical properties upon binding to nucleic acids.

Usually, the substituents on the naphthalimide ring could greatly affect various properties of naphthalimides, such as the optical properties, the interaction with nucleic acids and cell permeability. Most nucleic acid binding molecules usually bear at least one positive charge to enhance their binding affinity to nucleic acids. Amino groups and guanidine groups[12] are usually introduced to these molecules to obtain positive charges under physiological conditions. In this work, we focus on the effect of amine and guanidine side chains on the DNA binding, membrane permeability, nuclear localization and cytotoxicity of 4-aminonaphthalimides. Five 4-aminonaphthalimides attached with different amine and/or guanidine groups (DNE, DND, ENE, DNG and GNG) were synthesized. The optical properties, nucleic acid binding ability, cell permeability, cellular distribution and cytotoxicity of these molecules were compared.

Results and Discussion

Synthesis and Optical properties of 4-amino-1,8-naphthalimides

Amine groups carry a positive charge under physiological conditions, and also can participate in hydrogen bonding with the bases and backbone of nucleic acids, thus they are usually covalently attached on nucleic acids binding molecules to enhance the binding ability[13]. Guanidine group exhibits strong basicity and is positively charged over a wide pH range. The protonated guanidine group has five potential hydrogen bond donors and three hydrogen bond acceptors, capable of forming both electrostatic and directed hydrogen bond interactions with nucleic acids[13,14]. Therefore, in order to investigate the effects of side chains on the nucleic acid binding, cellular internalization, cellular localization and cytotoxicity of naphthalimides, aminoethyl, dimethylaminopropyl and guanidinoethyl groups were respectively linked to imine group and 4-position amino group of 4-amino-1,8-naphthalimide. Scheme 1 shows the synthetic route of the target molecules, named DNE, DND, DNG, ENE and GNG. 4-bromine-1, 8-naphthalanhydride was used as the raw material and was reacted directly with ethylenediamine and 3-dimethylaminopropylamine to obtain DNE, DND and ENE. Guanidine group was derived from amino group by two methods[12a,15] to obtain DNG and GNG.

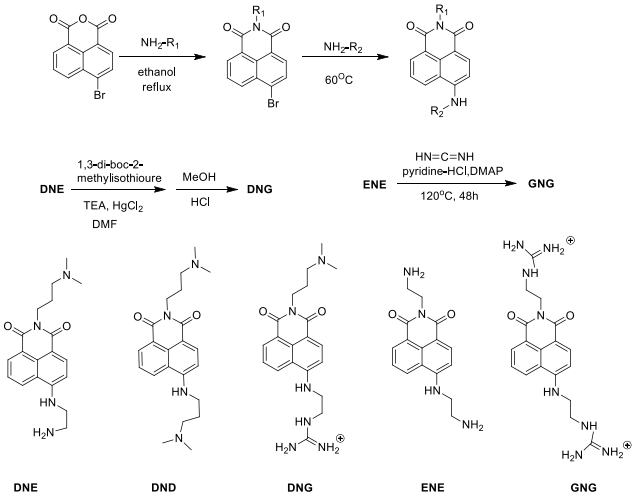

Scheme 1. Synthetic routes of DNE, DND, DNG, ENE and GNG.

Because of the amino groups or guanidino side chains, all these molecules can be dissolved in neutral aqueous solution at concentrations higher than 100 μM. Among them the molecules with guanidino groups, GNG and DNG, showed much higher solubility in water, but exhibited poor solubility in nonpolar solvent. The absorption spectra of these molecules in PBS all exhibited a single broad band with a maximum at 445 nm in visible region (Figure 1), which is the characteristic absorption of 4-aminonaphthalimide ring structure, suggesting that the side chains did not much affect their absorption spectra. Four of these molecules, DND, DNE, ENE and DNG exhibited similar emission spectra with maximum approximately at 540 nm in PBS. But GNG, bearing two guanidino groups exhibited an additional emission band (with maximum at 460 nm) besides the 540 nm band (Figure 1). The pH change in the range of 4.0-9.0 did not significantly influence the fluorescence spectra of these naphthalimides (Figure S1).

The fluorescence quantum yields (Φ_f) of these naphthalimides in different solvents were determined (Table S1) by using N-butyl-4-butylamine-1,8-naphthalimide (Φ_f = 0.70 in ethanol) as standard[16] It is noteworthy that the Φ_fs of these compounds in Phosphate buffered saline (PBS, pH 7.4) were similar (0.29-0.35), which suggest that we can compare the amount of these molecules in physiological salt environment by comparing their fluorescence intensity.

Nucleic acid binding of 4-amino-1,8-naphthalimides

The DNA binding properties of these molecules were investigated by UV-Vis absorption spectra and emission spectra. As shown in Figure 1, upon the addition of calf thymus DNA (CT-DNA), the absorption spectra of these molecules gradually decreased and accompanied with a slight red shift; and the emission spectra of these molecules gradually decreased and accompanied with a slight blue shift. These spectral changes were well consistent with that of other naphthalimides intercalators.[17] Based on the curves of decreasing rate of fluorescence intensity versus the concentration of CT-DNA, the binding ability of these 4-amino-1,8-naphthalimides to CT-DNA was compared by the concentration of DNA to induce a 50% of the maximal fluorescence decrease ($DC_{50\ DNA}$), i.e. GNG > DNG > DNE >

DND > ENE (Figure S2). It needs to be noted that the binding of these molecules to DNA only caused partial decrease (less than 40%) of their absorbance and emission, suggesting that these molecules can be used as fluorescent dyes for DNA staining.

The well-known nuclear staining dye DAPI can strongly bind to double-stranded DNA (ds-DNA) and lead to a strong emission enhancement; it prefers to bind A/T-rich DNA sequences by inserting into their narrow minor groove[18]. The fluorescence emission spectrum of DAPI (maximum at 461 nm) overlaps with the absorption spectra of naphthalimides, which may result in fluorescence resonance energy transfer (FRET) if DAPI and Naphthalimides bind on a DNA strand within a short distance. Based on this consideration, a FRET experiment was performed by excitation at 345 nm where naphthalimides showed very weak absorption and DAPI showed high absorption (Figure S3). As shown in Figure 2, DAPI exhibited weak fluorescence in the absence of DNA and exhibited very strong fluorescence upon binding to DNA; the addition of excess naphthalimides caused great decrease of the fluorescence of DAPI-DNA complex, and significant increase of the fluorescence of naphthalimides. There are two possible reasons for the fluorescence decrease of DAPI, DNA binding displacement by naphthalimides and FRET from DAPI to naphthalimides. In this experiment the concentrations of naphthalimides were much higher than DAPI and DNA, if the reason was binding displacement, most of DAPI should be displaced by naphthalimides; above results have shown that the DNA binding caused the fluorescence decrease of naphthalimides (Figure 1), the flurescence of naphthalimides should decrease. Therefore, the binding displacement that caused a substantial decrease of DNA-bound DAPI could be excluded; and the fluorescence decrease of DAPI and fluorescence increase of naphthalimide could be attributed to a FRET signal between DAPI and napthalimides. The further titration experiments with naphthalimides showed that the fluorescence of DAPI decreased with the increase of the concentration of naphthalimides (Figure S4). The concentration of naphthalimides to induce a 50% of the maximal fluorescence decrease of DAPI (DC_{50dye}) was estimated by the curves of DAPI fluorescence decrease versus the concentration of naphthalimides, which also indirectly reflected the binding ability of them to CT-DNA, i.e. GNG > DNG > DND > DNE >ENE. (Figure S5) This order of binding ability was similar with that obtained by fluorometric titrations with CT-DNA as shown above. This set of results suggests that these naphthalimides bind to DNA at a different site from DAPI.

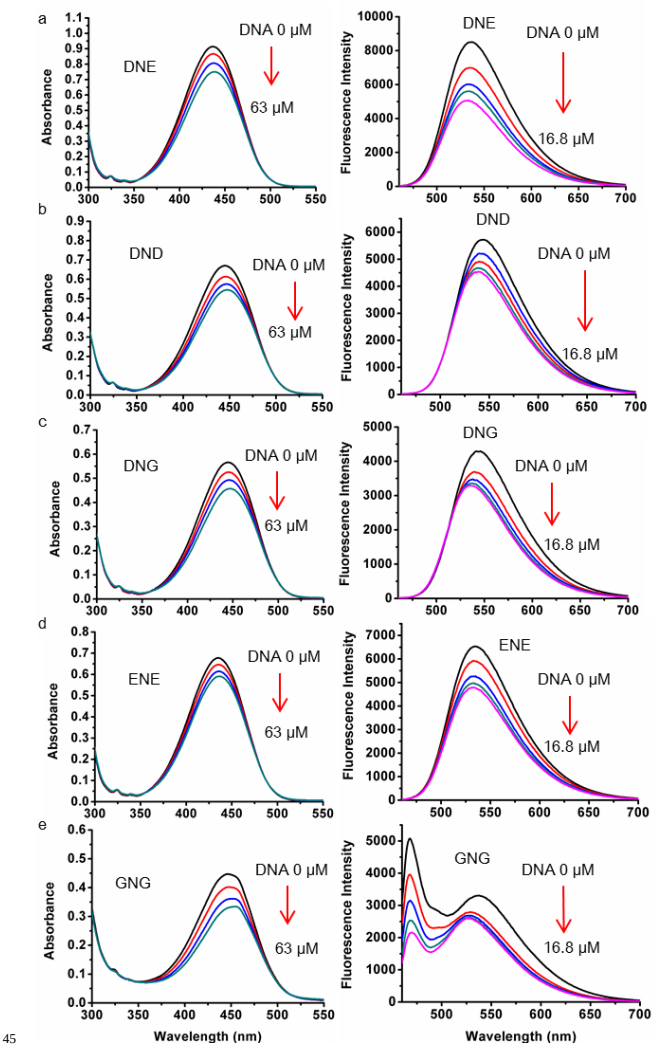

Figure 1. The changes of absorption (left) and emission (right) spectra in PBS buffer (pH 7.4) upon the addition of DNE, DND, DNG, ENE, GNG. For absorption spectra, [naphthalimides]: 50 μM, [CT-DNA]: 0, 21, 42, 63 μM (in base pairs); For emission spectra, [naphthalimides]: 2.0 μM, [CT-DNA]: 0, 4.2, 8.4, 12.6, 16.8 μM, exicited at 445 nm.

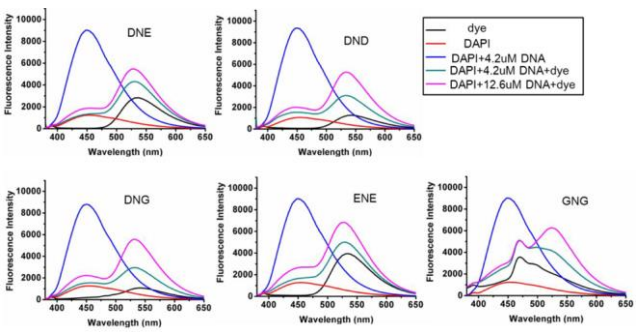

Figure 2. The fluorescence spectral change of DAPI and naphthalimides in the presence of CT-DNA (concentration is in base pairs). All data were collected in PBS buffer, pH 7.4 with excitation at 345 nm. [DNE], [DND], [DNG] and [GNG]:15 μM; [ENE]: 25 μM; DAPI: 1 μM.

Nucleic acid staining in agarose gel electrophoresis

In order to further demonstrate that the binding of DNE, DNG, ENE and GNG is strong enough for the nucleic acid staining, the gel electrophoresis experiments were performed. Different kinds

of nucleic acid sequences including ds-DNA, RNA and single-stranded DNA (ss-DNA) were premixed with these naphthalimides respectively; and the widely used fluorescent stains, EB and DAPI were chosen for positive control. As shown in Figure 3, green fluorescent bands of ds-DNA ladders (L1 and L2) and RNA stained by DNE, DNG, ENE and GNG were visualized under UV-light. But ss-DNA (A_{40}) could not be stained by these compounds. The resolution of the stained DNA ladders was similar or better than that stained by EB (red bands) or DAPI (blue bands). These results suggest that the high affinity complexes of ds-DNA and RNA with naphthalimides are stable enough and did not dissociate in the agarose gels during electrophoresis (pH 8.05). Although the fluorescence of these naphthalimides does not improve upon binding to DNA or RNA, the retention of ligand's most of the fluorescence intensity even after certain amount of quenching due to DNA interaction clearly demonstrates that they can be used as dyes for ds-DNA and RNA staining in gel electrophoresis.

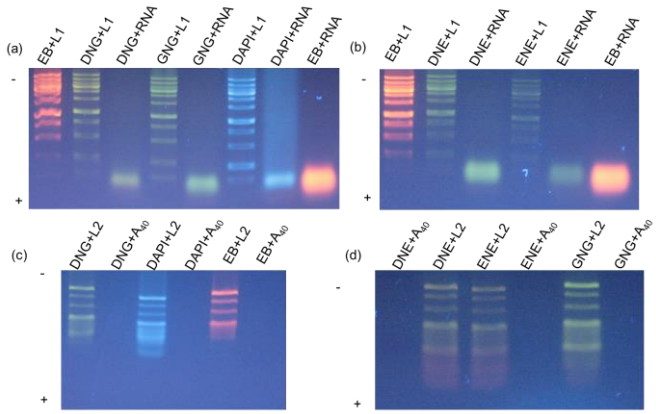

Figure 3. Gel electrophoresis analysis of different nucleic acids pre-stained by DNE, DNG, ENE and GNG. (a) long nucleic acids stained by DNG and GNG in 1% agarose gel. (b) long nucleic acids stained by DNE and ENE in1% agarose gel. (c) short nucleic acids stained by DNG in 2% agarose gel. (d) short nucleic acids stained by DNE, ENE and GNG in 2% agarose gel. The concentration of compounds, EB: 50 μM; DAPI, DNG, GNG, DNE, ENE: 40 μM. L1：1X DNA ladder1 (100-6000bp); L2: 1 X DNA ladder 2 (20-500bp). RNA: 2 mg/mL. A40: 10 μM. Loading volume 10 μL. Fluorescent bands were photographed under UV light.

Cell permeability of Naphthalimides

To compare the cell permeability of these dyes, they were incubated with MCF-7 cells at 37 ^{o}C and 4 ^{o}C, as well as with fixed cells for different time respectively. After washing with PBS, the fluorescence of cells was measured on flow cytometer (Figure S6), which represents the amount of dyes in cells. The median fluorescence intensities of cells are summarized in table 2. Because the membrane of fixed cells was penetrated by Triton X-100, dyes could freely enter cells. Therefore the fluorescence of fixed cells stained by dyes was much stronger than that of living cells except for that stained by DND. The order of the fluorescence intensity in fixed cells was GNG > DNG > DNE > DND > ENE, which is consistent with that of the binding ability of these dyes to DNA, suggesting that the binding to nucleic acid determine the amount of these dyes in fixed cells. For live cells, the fluorescence intensities of cells stained by DND and DNE at 37 ^{o}C were much higher than that of by other dyes. This result suggests that the dimethylaminopropyl (tertiary amino groups) favour the internalization of the naphthalimides. The fluorescence intensities of live cells stained by DND at 4 ^{o}C were much stronger than that by other dyes, even much stronger than that by DND incubated at 37 ^{o}C, suggesting that DND appear to cross the plasma membrane of cells through free diffusion. GNG and DNG has stronger binding ability to DNA than other dyes, but the fluorescence intensities of live cells stained by these two dyes were much weaker than that of by DND and DNE, suggesting that the guanidino group do not favour the internalization of naphthalimides. ENE has the lowest binding ability to DNA and also has weak cell permeability. It is worth to note that even the lowest fluorescence in the stained cells was several-fold higher than the background fluorescence of cells, suggesting that all the naphthalimides could enter live cells in certain extent.

Table 1. The median fluorescence of MCF-7 cells after stained by different naphthalimides (10 μM) under different conditions

Condition		Cell only	DNE	DND	DNG	ENE	GNG
Temp	Time						
37 ^{o}C	15 min	2.5	278	329	38.7	17.4	29.7
	30 min		671	869	52.6	60.6	46.2
	45 min		682	887	64	92.8	52.7
4 ^{o}C	15 min	3.53	54.8	1071	12.2	43.2	25.1
	30 min		90.1	1484	16.5	67.1	28.3
	45 min		114	1396	21.0	107	35.8
Fixed cells	10 min	2.06	885	589	2103	260	3955
	20 min		926	874	2488	309	4596
	30 min		1167	950	2502	367	5047

The cellular localization of naphthalimides

Unlike the nucleic acid probes that almost do not emit fluorescence until they interact with nucleic acids, the naphthalimides always emit fluorescence whether they bind to nucleic acids or not. Therefore the distribution of these molecules in cells can be observed by fluorescent imaging. In order to test whether these dyes can be used for nuclear imaging, DNG was first chosen to stain live cells and fixed cells. A popular cell-permeant nuclear stain, DAPI was chosen for co-staining. As shown in Figure 4a, after incubation at 37 ^{o}C for 30 min, both DAPI and DNG had entered living cells. The strong green fluorescence of DNG was observed in nuclei, and some weak green fluorescent spots were observed scattered in other regions, suggesting that DNG was concentrated in nuclei. The blue fluorescence of DAPI was mainly found in nuclei, that may due to the fluorescence turn-on property of DAPI upon binding to DNA. Similar results were also observed in cells stained by DNG at 4 ^{o}C for 30 min (Figure 4b). Although DNG showed much weaker cell permeability than DND, these results suggest that DNG has similar cell permeability with DAPI. The double staining by DAPI and DNG was also performed in fixed cells. The strong fluorescence from DNG and DAPI was observed in entire nuclei, only weak fluorescence from DNG was observed dispersed in other region of cells (Figure 4c). An interesting phenomenon was found in the double stained nuclei, i.e. some strongest stained regions by DNG (seen as green spots in Figure 4) were not stained by DAPI. These regions are considered as nucleoli, organelles that are responsible for the transcription and assembly of ribosomal RNA (rRNA) and made up of DNA, RNA and proteins.[19] This phenomenon also suggests that DAPI and DNG may bind to different sites of nucleic acids and DNG preferentially stain nucleoli.

To further investigate the cellular localization of these naphthalimides, all of them were incubated with live MCF-7 cells at 37 ^{o}C and 4 ^{o}C, and with fixed cells respectively. Considering the potential interference of DAPI on the binding or optical behaviour of naphthalimides, DAPI was not used this time. Because of the different cell permeability of these molecules, the images were collected at different PMT voltages to obtain optimal images. As shown in Figure 5, the fluorescence of all these dyes could be observed in cells, and mainly located in nuclei and especially in nucleoli, which are similar to the above results of double staining by DNG and DAPI. Among the stained live cells, the contrast between nuclei and cytoplasm stained by ENE was much weaker than that stained by other dyes, but the fluorescence in nucleoli was still strong enough to produce good contrast. Because dyes can freely enter the fixed cells, the fluorescence in nuclei of fixed cells was much stronger than that in live cells, but the fluorescence in cytoplasm was also bright, which reduced the contrast between nuclei and other regions. However, the fluorescence in nucleoli was still very strong. These results suggest that all these dyes mainly located in nuclei wherever in living or fixed cells. In addition, the further stronger fluorescence in nucleoli than other regions of nuclei suggests that all these naphthalimides can be used for nucleoli visualization when imaging the nuclei.

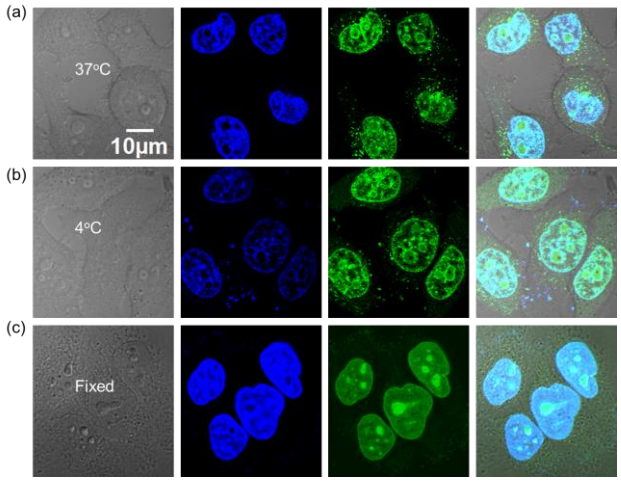

Figure 4. Double staining of MCF-7 cells with DNG and DAPI. (a) stained with 10 μM DNG and DAPI at 37 ^{o}C for 30 min. (b) stained with 10 μM DNG and DAPI at 4 ^{o}C for 30 min. (c) Fixed MCF-7 cells stained with 1 μM DAPI and 1.5 μM DNG at 4 ^{o}C for 15 min. Images from left to right: optical image; fluorescence image of DAPI (laser 405 nm); fluorescence image of DNG (laser 488 nm); overlay.

Dynamic fluorescent imaging of the internalization of DND and DNG

Since the green fluorescence of naphthalimides do not change much in different regions of cells, the cell internalization process of these dyes can be observed by confocal imaging. The flow cytometry results have shown that DND have good cell permeability, the internalization process of 10 μM DND was shown in Figure 6a and video 1 in the Supporting Information. Weak fluorescence was first observed on the cell membrane at 1 min, then fluorescence appeared in nuclei and continuously increased during 20 minutes; weak fluorescence in cytoplasm was also observed during this process but the increase was much slower than that in the nuclei. This suggests that DND internalized into cells following surface binding and then rapidly concentrated in nuclei. Since the cell permeability of DNG was much weak than DND, a higher concentration of DNG (20 μM) was used to investigate the internalization process of DNG. As shown in Figure 6b and video 2 in the Supporting Information, the green florescence was observed outside the cells at the beginning of incubation, then the green florescence appeared in nuclei at 2 min and became brighter continuously until 20 min, however, the fluorescence in cytoplasm was very weak in the first 5 minutes, and then became brighter, but was much weaker than that in nuclei all the time. The set of results suggest that DNG could internalize into cells, and bound to nuclei rapidly once it entered cells. All these results suggest that naphthalimides located in neuclei more specifically than other regions of cells.

Cite this: DOI: 10.1039/c0xx00000x

www.rsc.org/xxxxxx

ARTICLE TYPE

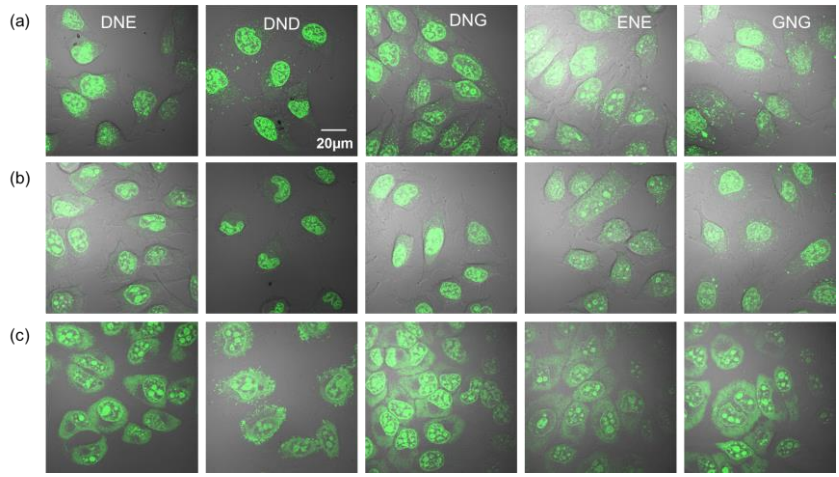

Figure 5. Fluorescence imaging of MCF-7 cells stained with 10 μM naphthalimides. (a) incubated at 37 °C for 30 min; (b) incubated at 4°C for 30 min; (c) fixed cells incubated with dyes at room temperature for 15 min.

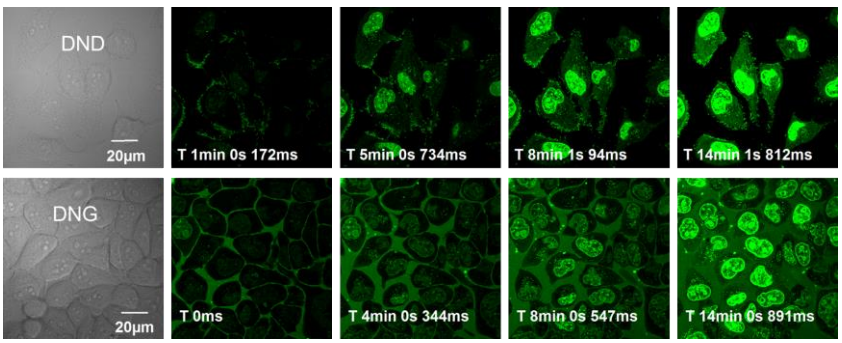

Figure 6. Real time fluorescence imaging: MCF-7 cells stained with 10 μM DND and 20 μM DNG at room temperature. DND staining was performed in pH 7.4 PBS buffer and DNG staining was performed in DMEM medium, pictures were collected every two min.

Cytotoxicity of of Naphthalimides

As DNA-intercalating agents, many naphthalimides have been explored as antitumor agents. Therefore the cytotoxicities of these naphthalimides to MCF-7 cells were tested to evaluate the effect of side chains on their cytotoxicity. As shown in Figure 7a, after a 24-h incubation at the concentration of 1 μM, only DND showed significant cytotoxicity; at the concentration of 5 μM, only DND and DNE showed significant cytotoxicity, which may due to the much higher cell permeability of DND and DNE than that of DNG, ENE and GNG. Further increasing the concentration, DND, DNE and ENE exhibited significant cytotoxicity (Figure 7b). The IC_{50} values of them were estimated to be 2.04±0.02, 10.41±0.12 and 56.62±0.08 μM. The cytotoxicities of these molecules were well consistent with their cell permeability. Although the interaction of these molecules with nucleic acids may be the direct reason of the cytotoxicity of these naphthalimides, the side chains of these molecules significant affect their cellular uptake, and result in very different cytotoxicity.

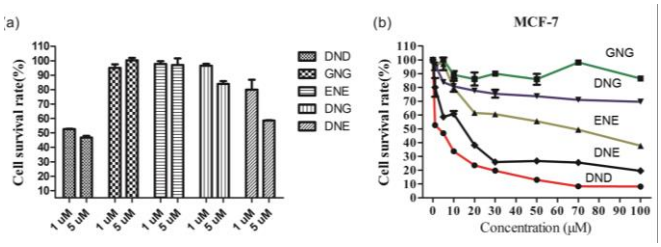

Figure 7. (a) Cytotoxicity of naphthalimides on MCF-7 cells at the concentrations of 1 and 5 μM. (b) Dose-response cytotoxicity of DND, GNG, ENE, DNG and DNE on MCF-7 cells, concentration of naphthalimides:1.0, 5.0, 10, 20, 30 50, 70 and 100 μM; data show the percentage of cell survival after incubated with naphthalimides for 24 h

Discussion

Above experiments compared the effects of different side chains on the optical properties, DNA binding, cell permeability, cellular localization, and cytotoxicity of 4-aminonaphthalimides. Because the amino groups and guanidine group were linked to 4-

aminonaphthalimide core through an alkyl chain with at least two C-atoms, the side chains did not significantly affect the absorption spectra of these naphthalimides, and did either not or only slightly affect their emission spectra except for GNG bearing two guanidinoethyl groups (Figure 1). The side chains were found to affect the binding ability of 4-aminonaphthalimides to nucleic acids. The naphthalimides bearing one or two guanidinoethyl groups (GNG and DNG) exhibited stronger binding ability than other naphthalimides bearing aminoethyl and/or dimethylaminopropyl groups. This can be attributed to the stronger hydrogen bonding ability to DNA, and the higher pK_a of guanidino group which is fully protonated at pH 7.4 as compared to amino group.

The flow cytometry assay suggested that the tertiary amine side chain facilitated the internalization of naphthalimides, and guanidino group was unfavourable to the internalization (Table 1). It well known that suitable lipophilicity is necessary for a molecule to pass through the lipid bilayer of the cell membrane. For the naphthalimides with tertiary amine side chain, the alkyl substitution on amino group suppressed the hydration of the cationic nitrogen and increased the lipophilicity. For GNG and DNG, the high degree of ionization of guanidino group made them exhibit low lipophilicity and hindered them freely pass through the cellular membrane. Cell imaging showed that all these naphthalimides mainly distributed in nuclei, suggesting that they have good selectivity to nucleic acids over proteins and lipids. Although, they did not show significant fluorescence change upon binding to nucleic acids, the strong binding ability to nucleic acids, relatively longer excitation/emission wavelength and good cell permeability make them alternative nuclear stains for live cell imaging.

Naphthalimides have been reported to possess high antitumour activity towards various tumour cells[8d]. The cytotoxicity experiment showed that the side chains significantly affected the cytotoxicity of the synthesized naphthalimides. The naphthalimides that have high cell permeability (DND and DNE) showed stronger cytotoxicity and the naphthalimides with higher binding ability to DNA (GNG and DNG) showed very weak cytotoxicity. It was well known that antitumor activity of one compound is determined by many factors including cell permeability, DNA binding ability, selectivity etc.. Although GNG and DNG had strong binding ability to DNA, the weak cell permeability greatly reduced their opportunity for the DNA binding in cells. Our results about the effects of side chains on these properties of 4-aminonaphthalimides provide useful information for the design of new antitumor drug.

Conclusion

Five 4-Aminonaphthalimides with aminoethyl, dimethylaminopropyl and guanidinoethyl side chains were synthesized. The absorption and emission spectral changes upon binding to DNA indicate that these naphthalimides bound to nucleic acids through intercalation between base pairs. The binding abilities of these naphthalimides were strong enough to visualize the prestained duplex DNAs and RNA during gel electrophoresis. The guanidinoethyl side chain was found to increase the binding ability of these naphthalimides. These naphthalimides could enter into live cells and mainly located in nuclei, especially in nucleoli, suggesting that these naphthalimides can serve as live-cell stains. The dimethylaminopropyl side chain benefited the cell permeability of 4-Aminonaphthalimides but guanidinoethyl side chain was unfavourable to the cell permeability. The naphthalimides bearing dimethylaminopropyl side chain exhibited strong cytotoxicity, but the naphthalimides with guanidinoethyl side chain showed weak cytotoxicity. These results suggest the possibility of changing the properties of naphthalimides by simply change their side chains, and provide useful information for the design of antitumor regents and fluorescent probes for cell imaging.

Experimental Section

The Synthesis and characterization of ENE, DNA, DNE, GNG, GND were shown in supporting information

Φ_f: fluorescence quantum yield

The fluorescence quantum yields of obtained derivatives in different solvents were determined on the basis of their absorption and fluorescence spectra. The N-butyl-4-butylamine-1,8-naphthalimide was used as standard with $\Phi_f = 0.70$ in ethanol. Where A_{ref}, F_{ref}, n_{ref} and A_{sample}, F_{sample}, n_{sample} represent the absorbance at the exited wavelength, the integrated emission band area and the solvent refractive index of the standard and the sample, it follows a formula like this:

$$\Phi_{sample} = \Phi_{ref} \times (A_{ref} \times F_{sample}) / (A_{sample} \times F_{ref}) \times (n^2_{sample} / n^2_{ref})$$

Optical Measurements

The absorption and fluorescence spectra were recorded in pH 7.4 PBS (phosphate buffered saline) buffer in a 1.0-cm quartz cuvette. For all the compounds used in the experiment, stoke solutions (1 mM and 10 mM) were prepared in DMSO, and kept at 4 ^{o}C. CT-DNA stock solution was prepared in Tris-HCl buffer (25 mM, pH 7.6), and kept at -20 ^{o}C. Absorption and fluorescence experiments were measured by titration with DNA into the buffer solution containing obtained derivatives.

Gel Electrophoresis

DNA dissolve in the pH 7.4 Tris-HCl buffer and RNA dissolve in the pH 7.4 Tris-HCl buffer containing DEPC. Prior to being loaded onto the agarose gel, dyes were incubated with DNA or RNA for 20 min at room tenperature. The naphthalimides, DAPI or EB were premixed with DNA or RNA in tris-HCl buffer (pH 7.4) for 20 min at room temperature and the mixed solution were loaded onto a 1% agarose gel or 2% agarose gel. The running buffer was 1X trisborate-ethylenediaminetetraacetic acid (TBE, pH 8.05) buffer. The gel was balanced for 10 min at 110 V, and then the electrophoresis was performed for about 40 min at 110 V. The Gels were exposed to UV light and photographed.

Confocal Imaging

MCF-7 (hormone-dependent breast cancer) cells were purchased from Cell Resource Center of Shanghai Institute for Biological Sciences (Chinese Academy of Sciences, Shanghai, China), and incubated in Dulbecco's Modified Eagle Medium (DMEM, Gibico) supplemented with 10% fetal bovine serum (FBS, Gibcio) and 1% penicillin/streptomycin (Hyclone). Cells

were cultured in a humidified incubator at 37℃ with 5% CO_2. For the purpose of staining and imaging, cells were seeded in a 35 mm × 12 mm style cell culture dish (Φ20 mm glass bottom) and cultured for 24 h (cell confluence must be over 80%). Cells fixation was conducted with 4% paraformaldehyde for 15 min and fixed cells were washed three times with PBS. Then 0.5% Triton X-100 PBS solution was added to permeabilize cells for 10 min, removed the solution and washed three times with PBS. The cells were incubated with naphthalimides and/or DAPI for different time at different temperature as indicated. After washed with PBS for three times, cells were imaged with an OLYMPUS FV1000-IX81 confocal laser-scanning microscope (Olympus Corporation, Japan), The fluorescence of DAPI was excited by 405 nm laser and collected from 425-475 nm; the fluorescence of naphthalimides was excited by 488 nm laser and collected from 500-600 nm. Florescent images (512 ×512 pixels) were observed using a 100 ×objective lens and the images were processed using the Olympus FV10-ASW 1.6 viewer software.

Flow cytometry assay

MCF-7 was seeded in 12-well plates (2×10^5 cells/well), and cultured for 24-48 h (cell confluence must be over 80%). Then cells were incubated with 10 μM naphthalimides for 15 min, 30 min and 45 min. Fixed cells treated as the confocal imaging experiment. After washed with PBS for three times, cells were detached by trypsin. Detached cells were washed with PBS for three times, filtrated with 100 μm cell strainer, and analysed with flow cytometer by counting 10000 events.

Cytotoxicity Assay

MCF-7 was seeded in 96-well plates (5×10^3 cells/well) and allowed to attach for 12 h before treatment. Then different concentrations of DNE, DNG, ENE, DND and GNG (1.0, 5.0, 10, 20, 30, 50, 70 and 100 μM) were added into cells respectively and further incubated for 24 h. Then the medium was replaced with 100 μL of fresh medium containing 10 μL of CCK-8 reagent (without FBS and penicillin/streptomycin). After incubation at 37 ℃ /5% CO_2 for 1 h, the absorbance at 450 nm was measured on a Spectra Max M5 (Molecular Devices, CA, USA). The cell viability rate (VR) was calculated according to the equation: $VR = (A-A_0)/(A_S-A_0) \times 100\%$, where A is the absorbance of the experimental group, As is the absorbance of the control group and A_0 is the absorbance of blank group (no cells).

Acknowledgements

We gratefully acknowledge the financial support from Grant 973 Program (2011CB935800, 2011CB911000 and 2013CB933700) and NSF of China (21275149, 21375135, 21205124 and 21321003).

Notes and references

[a] Beijing National Laboratory for Molecular Sciences, Key Laboratory of Analytical Chemistry for Living Biosystems, Institute of Chemistry, Chinese Academy of Sciences, Beijing, 100190, china.
E-mail: sgdh@iccas.ac.cn

[b] Graduate School of the Chinese Academy of Sciences, Beijing 100049, China

[c] The College of Chemistry of Xiangtan University, Xiangtan 411105, China

†Electronic Supplementary Information (ESI) available: [details of any supplementary information available should be included here]. See DOI: 10.1039/b000000x/

1 (a) L. J. Kricka, *Ann. Clin. Biochem.*, 2002, **39**, 114-129; (b) B. Maji, S.Bhattacharya, *Chem. Commun.*, 2014, **50**, 6422-6438.
2 (a) R. Palchaudhuri and P. J. Hergenrother, *Curr. Opin. Biotechnol.*, 2007, **18**, 497-503; (b) D. Roeland Boer and A. Canals, M. Coll, *Dalton Trans.*, 2009, **3**, 399-414.
3 (a) A. K. Jain, A. Paul, B. Maji, K. Muniyappa, S. Bhattacharya, *J. Med. Chem.*, 2012, **55**, 2981-2993; (b) A. K. Jain, V. V. Reddy, A. Paul, K. Muniyappa, S. Bhattacharya, *Biochemistry*, 2009, **48**, 10693-10704; (c) P. Chaudhuri, H. K. Majumder, S. Bhattacharya, *J. Med. Chem.*,2007, **50**, 2536-2540; (d) P. Chaudhuri, B. Ganguly, S. Bhattacharya, *J. Org. Chem.*, 2007, **72**, 1912-1923.
4 (a) K. Guenther and M. Mertig, R. Seidel, *Nucleic Acids Res.*, 2010, **38**, 6526-6532; (b) L. S. Ploeger, H. F. J. Dullens, A. Huisman and P. J. van Diest, *Biotech. Histochem.*, 2008, **83**, 63-69; (c) T. Suzuki, K. Fujikura, T. Higashiyama and K. Takata, J. Histochem. *Cytochem.*, 1997, **45**, 49-53; (d) D. R. G. Pitter, J. Wigenius, A. S. Brown, J. D. Baker, F. Westerlund and J. N. Wilson, *Org. Lett.*, 2013, **15**, 1330-1333.
5 X. Peng, T. Wu, J. Fan, J. Wang, S. Zhang, F. Song and S. Sun, *Angew. Chem. Int. Ed.*, 2011, **50**, 4180-4183.
6 C. Li, M. Yu, Y. Sun, Y. Wu, C. Huang and F. Li, *J. Am. Chem. Soc.*, 2011, **133**, 11231-11239.
7 P. J. Smith, N. Blunt, M. Wiltshire, T. Hoy, P. Teesdale-Spittle, M.R. Craven, J. V. Watson, W. B. Amos, R. J. Errington and L. H. Patterson, *Cytometry*, 2000, **40**, 280-291;
8 (a) M. F. Brana and A. Ramos, *Curr. Med. Chem. Anticancer Agents.*, 2001, **1**, 237-255; (b) L. Ingrassia, F. Lefranc, R. Kiss, T. Mijatovic, *Curr. Med. Chem.*, 2009, **16**, 1192-1213; (c) M. Lv and H. Xu, *Curr. Med. Chem.*, 2009, **16**, 4797-4813; (c) S. Banerjee, E. B. Veale, C. M. Phelan, S. A. Murphy, G. M. Tocci, L. J. Gillespie, D. O. Frimannsson, J. M. Kelly and T. Gunnlaugsson, *Chem. Soc. Rev.*, 2013, **42**, 1601-1618.
9 (a) I. Grabchev, I. Moneva, V. Bojinov and S. Guittonneau, *J. Mater. Chem.*, 2000, **10**, 1291-1296; (b) X. F. Guo, X. H. Qian and L. H. Jia, *J. Am. Chem. Soc.*, 2004, **126**, 2272-2273; (c) X. L. Li, Y. J. Lin, Q. Q. Wang, Y. K. Yuan, H. Zhang and X. H. Qian, Eur. *J. Med. Chem.*, 2011, **46**, 1274-1279; (d) J. Zhou, H. Y. Liu, B. Jin, X. J. Liu, H. B. Fu and D. H. Shangguan, *J. Mater. Chem. C*, 2013, **1**, 4427-4436.
10 (a) L. Duan, Y. Xu and X. Qian, *Chem. Commun.*, 2008, **47**, 6339-6341; (b) L. Duan, Y. Xu, X. Qian, *Chem. Commun.*, 2008, **47**, 39-6341; (c) X. Qian, Y. Xiao, Y. Xu, X. Guo, J. Qian, W. Zhu, *Chem. Commun.*, 2010, **46**, 6418-6436; (d) C. L. Fang, J. Zhou, X. J. Liu, Z. H. Cao, D. H. Shangguan, *Dalton Trans.*, 2011, **40**, 899-903; (e) B. Zhu, X. Zhang, Y. Li, P. Wang, H. Zhang, X. Zhang, *Chem. Commun.*, 2010, **46**, 5710-5712; (f) B. Zhu, C. Gao, Y. Zhao, C. Liu, Y. Li, Q. Wei, Z. Ma, B. Du, X. Zhang, *Chem. Commun.*, 2011, **47**, 8656-8658.
11 (a) D. Srikun, E.W. Miller, D.W. Dornaille, C. J. Chang, *J. Am. Chem. Soc.*, 2008, **130**, 4596-4597; (b) H. H. Lin, Y. C. Chan, J. W. Chen and C. C. Chang, *J. Mater. Chem.*, 2011, **21**, 3170-3177; (c) M. H. Lee, J. H. Han, P. S. Kwon, S. Bhuniya, J. Y. Kim, J. L. Sessler, C. Kang and J. S. Kim, *J. Am. Chem. Soc.*, 2012, **134**, 1316-1322; (d) J. Zhou, C. L. Fang, T. J. Chang, X. J. Liu and D. H. Shangguan, *J. Mater. Chem. B*, 2013, **1**, 661-667;
12 (a) K. Ohara, M. Smietana, A. Restouin, S. Mollard, J. P. Borg, Y. Collette and J. J. Vasseur, *J. Mater. Chem.*, 2007, **50**, 6465-6475; (b) R. Seliga, M. Pilatova, M. Sarissky, V. Viglasky, M. Walko and J. Mojzis, *Mol Biol Rep.*, 2013, **40**, 4129-4137; (c) V. Bagnacani, V. Franceschi, M. Bassi, M. Lomazzi, G. Donofrio, F. Sansone, A. Casnati and R. Ungaro, *Nat. Commun.*, 2013, **4**, 1721-1727.

13 M. F. Brana, M. Cacho, M. A. Garcia, B. de Pascual-Teresa, A. Ramos, M. T. Dominguez, J. M. Pozuelo, C. Abradelo, M. F. Rey-Stolle, M. Yuste, M. Banez-Coronel and J. C. Lacal, *J. Mater. Chem.*, 2004, **47**, 1391-1399.

14 (a) K. A. Schug and W. Lindner, *Chem. Rev.*, 2005, **105**, 67-113; (b) L. Chen, J. N. M. Glover, P. G. Hogan, A. Rao, S. C. Harrison, *Nature*, 1998, **392**, 42-48; (c) R. K. Arafa, M. A. Ismail, M. Munde, W. D. Wilson, T. Wenzler, R. Brun and D. W. Boykin, *Eur. J. Med. Chem.*, 2008, **43**, 2901-2908; (d) M. A. Ismail, R. K. Arafa, T. Wenzler, R. Brun, F. A. Tanious, W. D. Wilson, D. W. Boykin, *Bioorg. Med. Chem.*, 2008, **16**, 683-691; (e) W. Hu, C. Blecking, M. Kralj, L. Suman, I. Piantanida and T. Schrader, *Chemistry*, 2012, **18**, 3589-3597; (f) K. Ohara, M. Smietana and J. J. Vasseur, *J. Am. Soc. Mass. Spectrom.*, 2006, **17**, 283-291; (h) C. Bailly, R. K. Arafa, F. A. Tanious, W. Laine, C. Tardy, A. Lansiaux, P. Colson, D. W. Boykin and W. D. Wilson, *Biochemistry*, 2005, **44**, 1941-1952.

15 J. Alzeer, P. J. C. Roth and N.W. Luedtke, *Chem. Commun.*, 2009, **15**, 1970-1971.

16 V. Wintgens, P. Valat, J. Kossanyi, L. Biczok, A. Demeter and T. Berces, *J. Chem. Soc., Faraday Trans.*, 1994, **90**, 411-421

17 (a) L. Xie, Y. Xu, F. Wang, J. Liu, X. Qian and J. Cui, *Bioorg. Med. Chem.*, 2009, **17**, 804-810; (b) Z. Chen, X. Liang, H. Zhang, H. Xie, J. Liu, Y. Xu, W. Zhu, Y. Wang, X. Wang, S. Tan, D. Kuang and X. Qian, *J. Med. Chem.*, 2010, **53**, 2589-2600; (c)K. Faulhaber, A. Granzhan, H. Ihmels, D. Otto, L. Thomas and S. Wells, *Photochem Photobiol Sci.*, 2011, **10**, 1535-1545; (d) K. Wang, Y. Wang, X. Yan, H. Chen, G. Ma, P. Zhang, J. Li, X. Li and J. Zhang, *Bioorg. Med. Chem.*, 2012, **22**, 937-941; (e) P. Bhattacharya, D. Sahoo and S. Chakravorti, *J. Photochem. Photobiol.*, A, 2012, **250**, 25-32.

18 M. I. Sanchez, J. Martinez-Costas, F. Gonzalez, M. A. Bermudez, M. Eugenio Vazquez and J. L. Mascarenas, *ACS Chem. Biol.*, 2012, **7**, 1276-1280.

19 (a) I. Lubitz, D. Zikich and A. Kotlyar, *Biochemistry*, 2010, **49**, 3567-3574; (b) V. Sirri, S. Urcuqui-Inchima, P. Roussel and D. Hernandez-Verdun, *Histochem Cell Biol.*, 2008, **129**, 13-31.